



Constrained and UV-activatable cell-penetrating peptides for intracellular delivery of liposomes

Morten B. Hansen^a, Ethlenn van Gaal^b, Inge Minten^a, Gert Storm^{b,c},
Jan C.M. van Hest^a, Dennis W.P.M. Löwik^{a,*}

^a Radboud University Nijmegen, Institute for Molecules and Materials, Department of Organic Chemistry, Heyendaalseweg 135, 6525 AJ Nijmegen, The Netherlands

^b Department of Pharmaceutics, Utrecht Institute of Pharmaceutical Sciences, Utrecht University, David de Wiedgebouw, Universiteitsweg 99, 3584 CG Utrecht, The Netherlands

^c MIRA Institute for Biomedical Technology & Technical Medicine, Faculty of Science & Technology, University of Twente, Building Zuidhorst, 7500 AE Enschede, The Netherlands

ARTICLE INFO

Article history:

Received 20 April 2012

Accepted 9 October 2012

Available online 17 October 2012

Keywords:

Cell penetrating peptide

Liposomes

Peptide amphiphiles

Activatable cellular transduction

ABSTRACT

Herein we report on the development of a novel method of constraining a cell-penetrating peptide, which can be used to trigger transport of liposomes into cells upon in this case radiation with UV-light. A cell-penetrating peptide, which was modified on both termini with an alkyl chain, was anchored to the liposomal surface in a constrained and deactivated form. Since one of the two alkyl chains was connected to the peptide via a UV-cleavable linker, disconnection of this alkyl chain upon irradiation led to the exposure of the cell-penetrating peptide, and mediated the transport of the entire liposome particle into cells.

© 2012 Elsevier B.V. All rights reserved.

1. Introduction

Over the past decades, numerous drug carriers have been developed from a wide range of materials [1–12]. A common goal for most of these carriers is to address some of the inherent problems associated with administration of drugs, such as toxicity, instability and unfavorable biodistribution. To deal with these issues, encapsulation of the drug in a carrier is often the method of choice, as this serves to protect the drug from the body environment and *vice versa*, and to shift the biodistribution towards the target site hence the stability, safety and targeting efficiency of the drug can be increased. In this respect, liposomes have received a fair amount of attention as carriers of encapsulated drugs [13–16], because of their easy preparation (at lab scale), their composition of natural and relatively inexpensive starting materials, as well as approval of several liposome products by the FDA [17–19]. Of particular interest are the so-called Stealth liposomes, which are coated with poly(ethylene glycol) (PEG) to evade immune system interactions and thereby achieve a long circulation time in the bloodstream [20–24].

However, while encapsulation provides a solution for unfavorable biodistribution, toxicity and instability of drugs, encapsulated drugs on the other hand have to escape from the interior of the carrier to exert their activity. To gain control over this release, a plethora of triggers has been employed such as reduction [25,26], ultrasound [27,28], light [29–34], pH [6,35–40], temperature [41–43], magnetic [44] and enzymatic activity [2,45–47] to mediate drug release. Of these triggers,

pH, temperature and enzymatic triggers have been used to target drug carrier systems specifically to diseased tissues, as the latter areas often exhibit a decreased pH, elevated temperature or express specific enzymes [48]. The most precise control, however, is achieved when external triggers such as ultrasound, magnetism and light are employed since these can be applied to defined localized areas to induce drug release [49]. The disadvantage is that most of these externally applied triggers are restricted to superficial tissues, though deep-seated tissue may be reached with the aid of laparoscopy [49,50].

Up to now, most triggered-release carrier systems (including light-triggered systems) work *via* a destabilization of the carrier causing release of the encapsulated drug in the extra-cellular space. This, however, may lead to poor cellular uptake of the released drugs in the case of macromolecular and/or hydrophilic drugs, which do not easily cross the cell membrane (*e.g.* oligonucleotides) [51,52]. Hence, cellular uptake of the carrier *before* releasing its contents may be desirable. Regarding uptake, this can be facilitated by functionalization of the carrier with cell-penetrating peptides (CPPs), which is a class of peptides capable of inducing cellular uptake of almost any kind of cargo to which they have been attached [53–61]. However, modification of the liposome surface with Tat-peptides leads to aspecific interaction and uptake in non-target cells [62]. Moreover, its positive charge leads to the interaction with blood components and enhances clearance *via* the reticuloendothelial system [63], thereby compromising the stealth property that is essential for prolonged circulation. In order to combine stealth behavior and Tat-mediated cellular uptake, we designed a UV-activatable cell-penetrating peptide which is inactivated by means of constraining the peptide by ‘hiding’ it on the surface of a liposome. Reactivation of

* Corresponding author.

E-mail address: d.lowik@science.ru.nl (D.W.P.M. Löwik).

the peptide can be accomplished by releasing the constrain via UV-irradiation.

2. Materials and methods

Breipohl resin was purchased from Novabiochem and Fmoc-L-amino acids were from Bachem (Bubendorf, Switzerland) or Novabiochem (EMD Chemicals, Gibbstown, USA). Lipids were from Avanti Polar Lipids (Alabaster, USA) or Lipoid (Steinhausen, Switzerland). Atto655 was purchased from ATTO-TEC (Siegen, Germany). All other chemicals were purchased from Baker, Fluka or Sigma Aldrich and used as received. Mass spectra were recorded on a Bruker Biflex MALDI-TOF (Bruker Daltronik, Bremen, Germany). Lyophilization was achieved using an ilShin Freeze Dryer (ilShin, Ede, The Netherlands).

Hepes (99%) was obtained from Acros Organics BVBA (Geel, Belgium). Phosphate-buffered saline (PBS) was purchased from B. Braun (Melsungen AG, Melsungen); fetal bovine serum (FBS) was from Integro, Zaandam, The Netherlands, Trypsin/EDTA, Plain DMEM (Dulbecco's modification of Eagle's medium, with 3.7 g/L sodium bicarbonate, 1 g/L-L-glucose, L-glutamine) and antibiotics/antimycotics (penicillin, streptomycin sulfate, amphotericin B) were all from PAA Laboratories (Pasching, Austria).

Human epithelial ovarian carcinoma (HeLa) cells were kindly given by the Institute of Biomembranes (Utrecht University, The Netherlands).

2.1. General peptide synthesis

Peptides were synthesized on Breipohl resins [64,65] using a Labortec640 peptide synthesizer (Labortec, Bubendorf, Switzerland) and employing a standard Fmoc solid-phase peptide synthesis (SPPS) protocol [66]. Briefly, the resin was swollen in DMF for 20 min prior to use. The first and subsequent Fmoc groups were removed by washing the resin with piperidine in DMF (20%, v/v) and then shaking for 25 min with another portion of piperidine in DMF. The desired sequence of amino acids was coupled to the resin using Fmoc-L-amino acids (3.0 eq), diisopropylcarbodiimide (DIPCDI, 3.3 eq) and *N*-hydroxy benzotriazole (HOBt, 3.6 eq). Peptide couplings were followed to completion using the Kaiser test [67]. After the final Fmoc removal the resin was washed with DMF, CH₂Cl₂, *i*-PrOH, CH₂Cl₂, and Et₂O and air-dried for at least 2 h.

2.2. Synthesis of Tat

The following sequence was synthesized by standard SPPS, as described above: YGRKKRRQRRRC. Tat on Wang resin (204 mg, loading 0.59 mmol/g, 35.4 μmol peptide) was suspended in cleavage mixture (2 mL, trifluoroacetic acid/water/triisopropyl-silane/thioanisole 90:5:2.5:2.5) for 18 h. The free peptide was precipitated from Et₂O, redissolved in water and lyophilized yielding the crude peptide as a white powder. The crude peptide was purified by semi-preparative HPLC affording Tat as a white powder after lyophilization (20 mg, 33%). MALDI-TOF [M + H] + *m/z*: 1718.3 (calcd. 1718.0).

2.3. Synthesis of Tat (R>A)

The following sequence was synthesized by standard SPPS and cleaved off the resin as described above: YGAKKARQRAGC. Tat (R>A) resin (140 mg, loading 0.59 mmol/g, 29.7 μmol peptide) afforded Tat (R>A) as a white powder after HPLC purification (6 mg, 13%). MALDI-TOF [M + H] + *m/z*: 1463.3 (calcd. 1462.8).

2.4. C12-UV-Tat (7a)

Tat on Breipohl resin (200 mg, loading 0.59 mmol/g, 34.7 μmol peptide) was suspended in DMF for 5 min, then DMF was removed

and the resin re-suspended in fresh DMF. DMAP (5 mg, 40.9 μmol) and activated nitro-benzyl alcohol **4a** (106 mg, 50.3 μmol) were added and the suspension was shaken in the dark over night. Then the resin was washed with DMF, CH₂Cl₂, *i*-PrOH, CH₂Cl₂ and Et₂O and suspended in the cleavage mixture (2 mL, trifluoroacetic acid/water/triisopropyl-silane/thioanisole 90:5:2.5:2.5) for 18 h. The free peptide was precipitated from Et₂O, redissolved in water and lyophilized yielding the crude peptide as a white powder. The crude peptide was purified by semi-preparative HPLC affording C12-UV-Tat **7a** as a white powder after lyophilization (20 mg, 27%). MALDI-TOF [M + H] + *m/z*: 2109.9 (calcd. 2108.2), fragment at 1778.4 and 1718.9 (the UV-cleavable linker was cleaved by the MALDI laser).

2.5. C16-UV-Tat (7b)

The title compound was prepared as described above for C12-UV-cleavable anchor Tat **7a** from Tat resin (333 mg, loading 0.59 mmol/g, 57.8 μmol peptide), activated benzyl alcohol **4b** (186 mg, 317 μmol) and DMAP (5 mg, 40.9 μmol) affording C16-UV-Tat **7b** as a white powder after lyophilization (81 mg, 65%). MALDI-TOF [M + H] + *m/z*: 2165.3 (calcd. 2164.3), fragment at 1787.7 and 1718.2 (the UV-cleavable linker was cleaved by the MALDI laser).

2.6. C12 Tat (8a)

Tat on Breipohl resin (300 mg, loading 0.59 mmol/g, 52.1 μmol peptide) was suspended in DMF for 5 min, then DMF was removed and the resin re-suspended in fresh DMF. Dodecanoic acid (75 mg, 337 μmol), DIPEA (120 μL, 1.25 mmol) and benzotriazole-1-yl-oxy-tris-(dimethylamino)-phosphonium hexafluorophosphate (BOP; 155 mg, 350 μmol) were added and the suspension was shaken over night. Then the resin was washed with DMF, CH₂Cl₂, *i*-PrOH, CH₂Cl₂ and Et₂O and suspended in cleavage mixture (2 mL, trifluoroacetic acid/water/triisopropylsilane/thioanisole 90:5:2.5:2.5) for 18 h. The free peptide was precipitated from Et₂O, redissolved in water and lyophilized affording a white powder. The crude peptide was purified by semi-preparative HPLC affording C12-Tat **8a** as a white powder after lyophilization (10 mg, 10%). MALDI-TOF [M + H] + *m/z*: 1900.3 (calcd. 1900.2).

2.7. C16 Tat (8b)

The title compound was prepared as described above for C12 Tat **8a** from Tat on Breipohl resin (300 mg, loading 0.59 mmol/g, 52.1 μmol peptide), hexadecanoic acid (87 mg, 339 μmol), DIPEA (120 μL, 1.25 mmol) and BOP (155 mg, 350 μmol) affording C16 Tat **8b** as a white powder (20 mg, 19%). MALDI-TOF [M + H] + *m/z*: 1957.4 (calcd. 1956.2).

2.8. Optimization of irradiation time

A solution of Atto655 (22.5 μg/mL) was prepared in HEPES buffer. This corresponds to the expected concentration in the liposome preparations assuming a statistical encapsulation of the dye. This solution was irradiated with a Bluepoint2 UV-lamp (Dr. Hönle, München, Germany) placed directly above the quartz cuvette containing the solution for the following time intervals: 0 s, 15 s, 30 s, 1 min, 2 min, 3 min, 4 min and 5 min. After each irradiation step a fluorescence spectrum was acquired on a LS55 fluorescence spectrometer (PerkinElmer, Groningen, The Netherlands) using the following settings: excitation at 600 nm, excitation slit 5.0 nm, emission slit 7.0 nm, scan range 620–850 nm, and scan speed 100 nm/min. Unless stated otherwise irradiation, when required, was performed for 2 min throughout this work.

2.9. Liposome preparation

The liposomes were prepared *via* the reversed-phase evaporation method [68] as follows: egg-derived hydrogenated phosphatidylcholine (62 mg, 81.4 μmol), 1,2-distearoyl-SN-glycero-3-phosphoethanolamine-N-[methoxy(polyethylene glycol)-2000] (12.5 mg, 4.5 μmol), 1,2-distearoyl-sn-glycero-3-phosphoethanolamine-N-[maleimido(polyethylene glycol)-2000] (13.3 mg, 4.5 μmol) and cholesterol (17 mg, 44.0 μmol) were dissolved in CHCl_3 (6.66 mL). A solution of Atto655 (0.8 mL, 0.5 mg/mL) was added as well as 10 mM HEPES buffer (4.54 mL, 10 mM HEPES, 1 mM EDTA, 0.8% NaCl, pH 7.5). The resulting two-phase system was vortexed to form a blue emulsion. The majority of the CHCl_3 was removed *in vacuo* and the remaining removed by flushing with N_2 . Vortex with a few glass beads was performed to aid formation of a homogeneous colloidal suspension. Water (0.5 mL) was added to compensate for loss during evaporation. The suspension was extruded through polycarbonate filters (3×600 nm and 6×200 nm) using a Lipex high-pressure extruder (Northern Lipids, Vancouver, Canada) and the size of the resulting liposome suspension was evaluated by dynamic light scattering (Zetasizer Nano-S, Malvern Instruments, Malvern, UK). A diameter of 194 nm and a polydispersity index of 0.11 were found (average of three measurements).

2.10. Functionalization of liposomes and zeta-potential determination

The freshly prepared liposome suspensions were split in seven equal aliquots. To each of six aliquots (one aliquot was saved as a control) was added a solution in HEPES buffer (100 μL) of the peptide (1.0 eq. relative to maleimido-groups) to be conjugated to the liposomes and a solution of tris(2-carboxyethyl)phosphine (10 μL , 0.5 M) was added. The reactions were shaken 1 h at rt, then 1 h at 40 °C and finally incubated at 4 °C over night. The liposome suspensions were diluted with HEPES buffer and ultracentrifuged for 40 min at 50,000 rpm and 4 °C (Sorvall Discovery-100, Thermo Scientific, Breda, The Netherlands). The resulting pellets were resuspended in HEPES buffer (500 μL). The zeta-potential of the liposome preparations was measured on a Malvern Zetasizer Nano-Z (Malvern Instruments, Malvern, UK) on liposome samples (50 μL) diluted into water (1.5 mL). The reported value is an average of three measurements.

2.11. Phosphate concentration determination

The phosphate concentration was determined according to Rouser's method [69]. Briefly, a standard dilution series of NaH_2PO_4 was set up in triplicate (0–160 μL of a 0.5 mM NaH_2PO_4 solution) and treated the same way as the samples (triplicate). The samples were dried at 180 °C, then perchloric acid (0.3 mL, 70%) was added to each, and the samples were incubated at 180 °C. Water (1.0 mL), a solution of $(\text{NH}_4)_6\text{Mo}_7\text{O}_{24}$ (0.5 mL, 1.2% w/v) and ascorbic acid (0.5 mL, 5% w/v) were added to each sample and these were incubated at 100 °C for 5 min. The absorbance at 797 nm was measured after cooling with cold water. The phosphate concentration could then be determined by means of the standard dilution series.

2.12. Analysis of cellular uptake by flow cytometry

HeLa cells were grown in DMEM supplemented with antibiotics/antimycotics and 10% heat-inactivated FBS. Cells were maintained at 37 °C in a 5% CO_2 humidified air atmosphere and split twice weekly. Cells were confirmed to be free from mycoplasma by periodical testing with a MycoAlert® Mycoplasma Detection Kit (Lonza, Verviers, Belgium).

Cells were harvested by trypsin/EDTA treatment, counted and diluted in cold medium to a concentration of 10^6 cells/mL. Liposome samples were diluted to 1 mM or 0.5 mM in PBS and 100 μL liposome sample was pipetted in triplicate into a 96-well plate. 100 μL cell suspension was added to the liposome suspensions and incubated 1 h at

4 °C protected from light. Samples were centrifuged for 5 min at $250 \times g$ at 4 °C. After removal of the supernatant, cells were washed with ice-cold PBS (3×200 μL , each centrifugation step at $250 \times g$ for 5 min at 4 °C). Cells were resuspended in 200 μL ice-cold PBS and kept on ice until time of analysis. Flow cytometric analysis was performed on a FACSCantoII (Becton and Dickinson, Mountain View, CA, USA) equipped with a 488 nm 20 mW Solid State diode laser and a 633 nm 20 mW HeNe laser. 10,000 cells were recorded per sample to determine Atto655 signal (APC/Cy7 channel).

2.13. Confocal laser scanning microscopy

The cellular uptake experiments were done with HeLa cells, which were seeded one day before the experiment in 8-well microscopy chambers (Nunc, Wiesbaden, Germany) at a density of 40,000 cells/well. At the time of the experiment, cells had grown to approximately 50% confluence. The liposome samples (100 nmol phosphate equivalents – typically around 10 μL) were diluted with Dulbecco's Modified Eagle Medium supplemented with 10% fetal calf serum (DMEM, 380 μL) and added to the cells, which were incubated for 2 h at 37 °C. The cells were washed with DMEM (3×400 μL) and imaged immediately. Confocal laser scanning microscopy was performed using a Leica Microsystems TCS SP2 AOBS system (Mannheim, Germany). Excitation of Atto655 was achieved with an argon laser [488 nm (52%), 514 nm (65%) and 561 nm (63%)] and the resulting emission was acquired between 575 and 800 nm as an average of four scans.

2.14. Dynamic light scattering of liposomes in medium

The liposome samples (100 nmol phosphate equivalents – typically around 5 μL) were diluted with DMEM, HEPES (200 μL) or HEPES supplemented with bovine serum albumin (200 μL , 4 mg/mL) and measured by dynamic light scattering. The DMEM and HEPES supplemented with bovine serum albumin solutions were also measured.

3. Results and discussion

As CPP, we used a Tat peptide derived from HIV [70,71], and imposed the UV-activatable property on the Tat peptide by incorporating it into a loop anchored to the surface of a PEG-ylated liposome *via* two alkyl-chains of which one contained a UV-cleavable linker (Fig. 1). While being in this loop, the surface PEG-chains shield the CPP from cells and thus enable stealth behavior and oppose interaction with target cells and thereby cellular uptake of the liposome. However, once in vicinity of target cells, irradiation can be applied to cleave the anchor, followed by loop-opening and exposure of Tat,

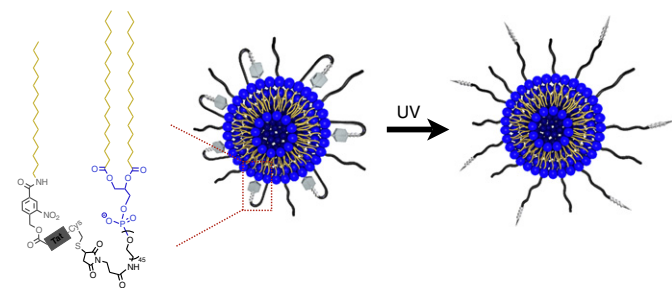


Fig. 1. Schematic overview of the UV-activatable Tat-liposome delivery system. A cell-penetrating peptide, Tat, is incorporated in a PEG-loop and anchored to the surface of a liposome with two lipid anchors, of which one can be cleaved by UV-light. Upon irradiation, the UV-cleavable anchor is cleaved leading to opening of the loop and exposure of the Tat-peptide. This enables uptake of the liposome as a result of the Tat-peptide being able to interact with cells. Dark gray box = Tat-peptide, light gray = UV-cleavable linker, black = PEG, yellow = fatty acids and blue = phosphate head groups.

which can now bind to cells and mediate the cellular internalization of the entire liposome particle.

Hence, to incorporate Tat in a surface-anchored loop on a liposome two alkyl anchors are required – a C-terminal and an N-terminal one. C-terminal anchoring was achieved via conjugation of a C-terminal cysteine thiol (introduced in Tat for this purpose) to a maleimide-PEG2000 functionalized distearoyl phosphatidylethanolamine, which was introduced into the liposomes during their preparation (see [Materials and methods](#)). In this regard, liposomes containing 10 mol% PEG of which 5 mol% were terminated with a maleimide group were found to be optimal for Tat-functionalization [56,72]. N-terminal anchoring was achieved by coupling either a UV-cleavable or non-cleavable anchor to the N-terminus of the Tat-peptide to afford a UV-activatable and non-activatable Tat-peptide, respectively (see below). In addition, two alkyl-chains with different lengths (C12 or C16) were used to prepare the UV-cleavable (C12-UV-Tat and C16-UV-Tat) and non-cleavable anchors (C12-Tat and C16-Tat) to provide insight into the influence of the alkyl chain-length on anchoring into the liposome.

3.1. Synthesis of the UV-cleavable anchor and its coupling to Tat

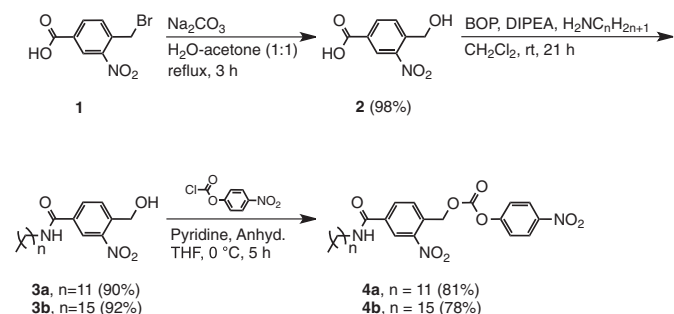
Two UV-cleavable anchors with different alkyl lengths (C_{12} and C_{16}) were synthesized from a common and commercially available starting material, 4-(bromomethyl)-3-nitrobenzoic acid **1** (Scheme 1).

First, the bromide was substituted with a hydroxy group under basic, aqueous conditions affording 4-(hydroxymethyl)-3-nitrobenzoic acid **2** in excellent yield [73]. Next, two different alkyl anchors were introduced by coupling either dodecylamine or hexadecylamine to the carboxyl group using BOP (benzotriazole-1-yl-oxy-tris-[dimethylamino]-phosphonium hexafluorophosphate) as a coupling reagent providing anchor **3a** and **3b** in good yields. Subsequently, the two anchors **3a** and **3b** were activated with 4-nitrophenyl chloroformate for coupling to the Tat peptide (Scheme 2).

The Tat peptide was prepared via solid phase peptide synthesis on a Wang-resin using standard Fmoc chemistry [66]. After the final Fmoc removal with 20% piperidine in DMF, the activated anchors **4a** and **4b** were coupled to the free N-terminus using DMAP as a catalyst. A negative Kaiser-test [67] confirmed that the coupling was complete. Global deprotection and cleavage of the peptides **6a** and **6b** from the solid support were achieved by suspension of the immobilized peptides in trifluoroacetic acid. After removal of the resin by filtration, the crude peptides were precipitated in diethyl ether, air-dried, lyophilized and purified by HPLC affording the UV-anchor-Tat peptides **7a** and **7b**.

3.2. Synthesis of Tat peptides with non-cleavable anchors

Tat peptides with non-cleavable C_{12} and C_{16} anchors were synthesized and included in this study as negative controls, as these peptides were expected to form loops, which cannot be opened by UV-irradiation. Tat peptides with C_{12} and C_{16} anchors were synthesized by coupling lauric acid and palmitic acid, respectively, to the free N-terminus of Tat using



Scheme 1. Synthesis of the UV-cleavable anchors.

BOP as a coupling reagent. Completion of the coupling reaction was confirmed with a Kaiser-test and the peptides were cleaved off their resins and treated as described above.

3.3. Coupling of peptides to liposomes

Liposomes were prepared from egg-derived phosphatidylcholine and 10 mol% PEG2000-distearoyl phosphatidylethanolamine of which half of the PEG chains was terminated with maleimide and half with a methoxy group [56]. The Tat peptides with UV-cleavable and non-cleavable anchors were coupled to maleimide-functionalized liposomes via their C-terminal cysteine residue (Fig. 2A). In addition, Tat and Tat with three Arg → Ala mutations (Tat R>A) both without alkyl anchors were included as a positive and negative control respectively. Coupling of the peptides to the liposomes was evaluated by measuring the zeta-potential of the liposomes (Fig. 2B).

Unfunctionalized liposomes have a negative zeta-potential in water because of the presence of negatively charged phosphate head groups. However, after coupling of the positively charged Tat peptides to the liposomes all, except the Tat mutant (Tat R>A), had a positive zeta-potential, which indicated that the couplings were successful. The Tat mutant, on the other hand, yielded liposomes, which still had a negative zeta-potential although less negative than unfunctionalized liposomes. This might be due to the smaller positive net charge on the mutant Tat, though a less efficient coupling cannot be ruled out.

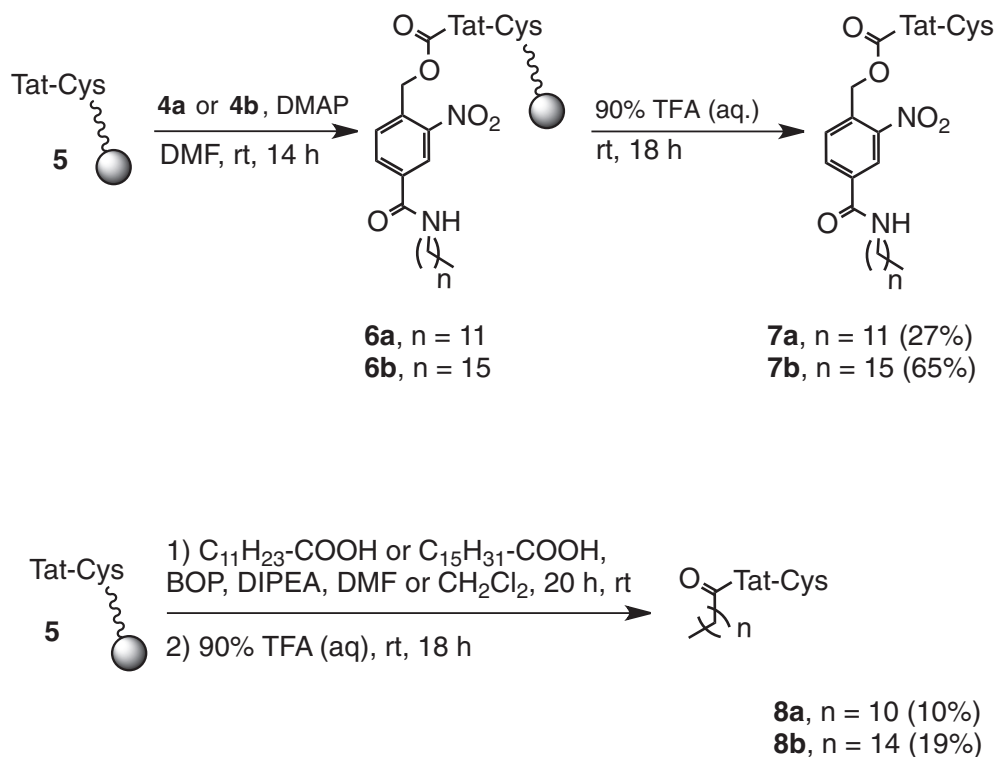
3.4. Cell-adhesion and uptake of Tat-liposomes

The cellular uptake of all Tat-liposome conjugates were investigated via flow cytometry analysis using an encapsulated Atto655 dye as fluorescent marker (Fig. 3). In this regard, irradiation experiments (supplementary data) showed that a 2 min irradiation period was a good optimum for sufficient cleavage of the UV-cleavable anchor without bleaching the Atto655 dye too much; hence a 2 min irradiation period was used whenever UV-mediated cleavage was required.

No unspecific adhesion was observed for unfunctionalized liposomes (negative control), whereas substantial and dose-dependent adherence was observed for Tat-modified liposomes (lip-Tat). Lip-Tat (R>A) showed limited cellular uptake (Fig. 3). Importantly, cellular uptake of lip-Tat-UV-C16 was marginal before irradiation. However, after irradiation cell-adhesion increased more than 10-fold (more than 15-fold, when corrected for photo-bleaching) to the same high level as observed for lip-Tat (positive control). The same trend was evident in the cellular uptake of the liposomes as demonstrated by confocal microscopy (Fig. 4). This clearly showed cellular uptake of lip-Tat but barely any uptake of lip-Tat (R>A), and unfunctionalized liposomes were undetectable. It should be noted, that the decreased adhesion of Tat-liposomes observed after irradiation is merely a result of photo-bleaching and does not reflect an actual decrease in adhesion. Together, this implies that the cell-adhesion and uptake observed for the series of Tat-liposomes is indeed mediated by functional Tat-peptides on the liposomes.

Labeling of the cell membrane with CellMask showed some co-localization with the liposomal dye (Atto655) suggesting that some of the liposomes were adhered to the cell membrane and not internalized. However, a large part of the liposomes were found inside the cells and separate from the membrane label, serving as a proof that these liposomes are indeed taken up by the cells.

A strong cell-adhesion before and after irradiation was also, but unexpectedly, observed for lip-Tat-C12 and lip-Tat-C16 as well as lip-Tat-UV-C12 showed strong cell-adhesion before irradiation, suggesting that shielding of the Tat-peptide was incomplete in these cases. However, inspection of the corresponding confocal images revealed the presence of large aggregates on the surfaces of the cells in the case of lip-Tat-C12 and lip-Tat-C16 and modest aggregation in the case of lip-Tat-UV-C12. In all these cases, the cells also seemed to be less viable (as discerned by



Scheme 2. Coupling of UV-cleavable and non-cleavable anchors to Tat (Tat = YGRKKRRQRRRG).

the transmission images) than cells treated with the other Tat-liposome conjugates. This implies that the observed cell-adhesion should not be considered as a simple adhesion of the Tat-liposomes to the cells but rather be regarded as the *propensity to aggregate* caused by incomplete loop insertion of the N-alkyl chain into the liposome membrane, leading to sedimentation of liposomes on cells rather than specific adherence and uptake. Interestingly, this propensity seemed to decrease going from lip-C12-Tat to lip-C16-Tat to UV-lip-C12-Tat suggesting that the

hydrophobic driving force for spontaneous insertion of the N-alkyl anchor into the liposome membrane increases along this series. In the case of lip-Tat-UV-C12, a substantial part of the Tat peptide was effectively shielded in the loop conformation, as this system exhibited an increased cell-adhesion after irradiation (even without taking photo-bleaching into account). The improved shielding observed for lip-Tat-UV-C12 implies that the aromatic ring in the UV-cleavable anchors provides a considerable additional hydrophobic driving force for loop-formation. Indeed, the lip-Tat-UV-C16, containing both the aromatic ring and the longer alkyl-chain showed the most efficient anchoring as can be inferred from the superior irradiation-triggered increase in cellular uptake upon irradiation.

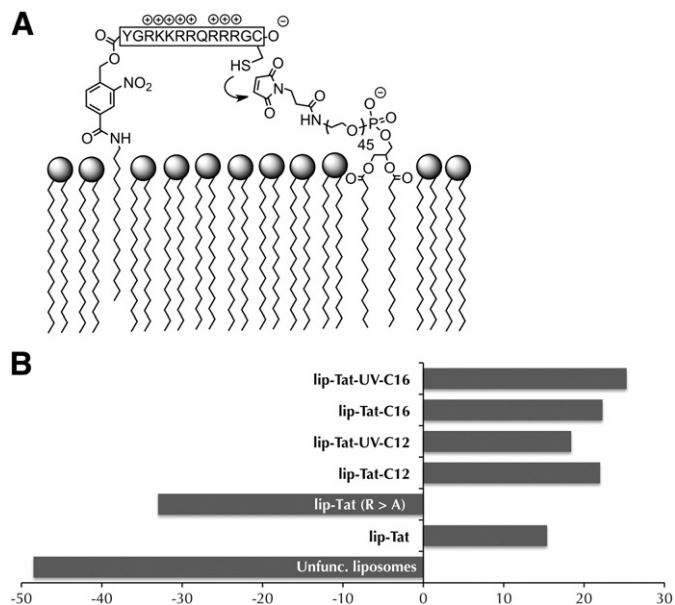


Fig. 2. Coupling of the Tat-peptides to liposomes. A) The Tat-peptides were coupled via a C-terminal cysteine residue and a liposome-PEG-maleimide group. B) Because of the positive charge of the Tat-peptides the coupling can be assessed as an increase in the zeta-potential of the liposomes.

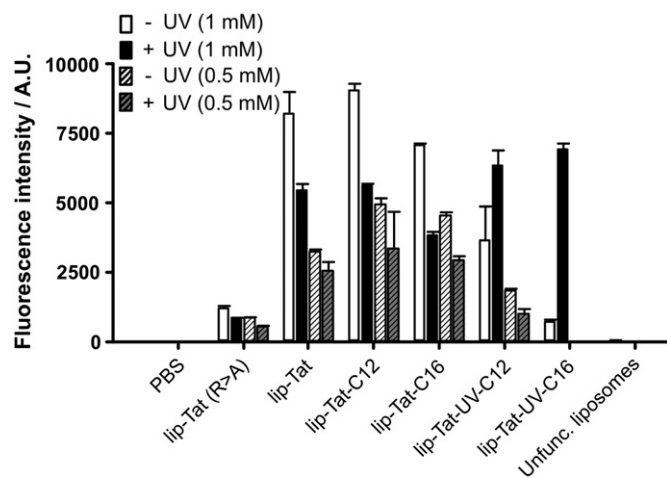


Fig. 3. Cellular uptake of Tat-liposomes. Flow cytometry study of the cellular uptake of the different Tat-liposomes before and after irradiation. Two different concentrations of liposomes were used – 0.5 and 1 mM (phosphate equivalents) – except for UV C16 for which only 1 mM was measured.

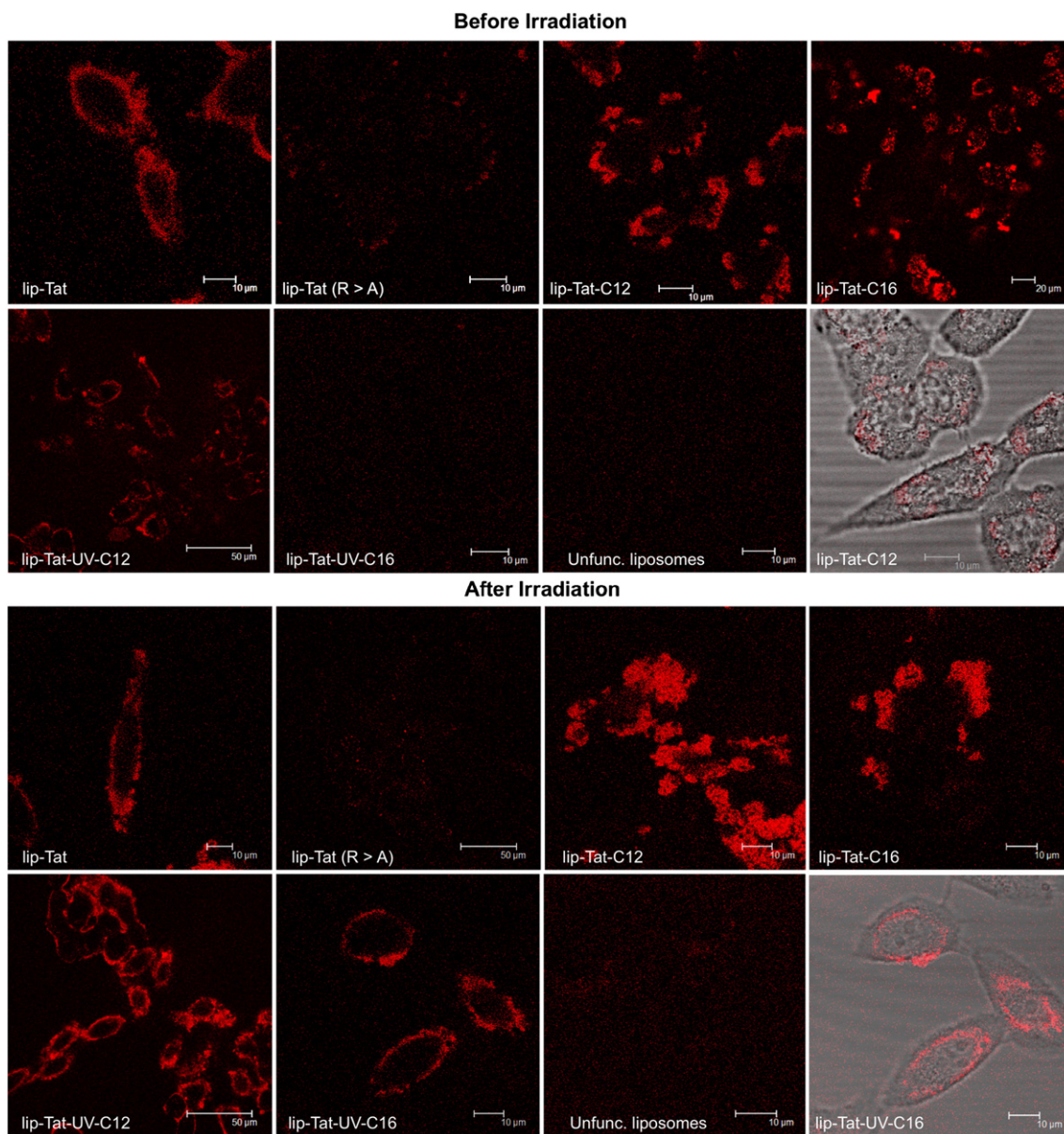


Fig. 4. Cellular uptake and adhesion. The cellular uptake and adhesion of the different Tat-liposomes was studied by confocal laser scanning microscopy before (top) and after irradiation (bottom). The liposomes were visualized by means of the encapsulated dye, Atto655 (red color). Transmission-fluorescence overlay images of cells treated with lip-Tat-C12 (top, lower right corner) and lip-Tat-UV-C16 (bottom, lower right corner) are included as examples (overlay images of all experiments can be found in the Supplementary data).

3.5. Dynamic light scattering – aggregation of liposomes

To shed light on the aggregation behavior of the Tat-liposomes their sizes were monitored by dynamic light scattering (DLS) in buffer and in cell medium. In HEPES buffer all liposomes had the expected mean size of approximately 175 nm, though lip-Tat-UV-C16 and lip-Tat-C16 showed a somewhat broader size distribution ($PDI < 0.25$; Fig. 5).

However, when the same DLS measurements were conducted in cell medium, lip-Tat-C12- and lip-Tat-UV-C12 liposomes increased markedly in size thus serving as a strong indication that the medium is responsible for the aggregation observed in the confocal microscopy experiments. For lip-Tat-C16 the already broad size distribution makes it difficult to draw firm conclusions about their aggregation behavior, though it seems that the size of these liposomes does not increase as much as observed for lip-Tat-C12. Because the medium

used in the experiments is rich in bovine serum albumin (BSA), it was speculated that this might play an important role in the aggregation process. In serum, the function of BSA is to bind fatty acids (to solubilize these), so it is reasonable to expect that BSA can bind to N-alkyl chains that failed to insert into the liposome membrane. Since BSA has six fatty acid binding sites [74] cross-linking and aggregation of liposomes with non-inserted N-alkyl chains would be possible. To test this hypothesis, lip-Tat-C12 were diluted into a HEPES buffer containing BSA at the same concentration as in the medium. Immediately, the solution turned turbid and DLS showed the presence of big particles (Fig. 5) strongly suggesting that BSA is profoundly involved in the aggregation observed in confocal microscopy possibly by binding to the non-inserted N-alkyl chains.

Lip-Tat-UV-C16, on the other hand did not increase in size at all neither in HEPES buffer nor in medium indicating that the loop-formation is complete in case of lip-Tat-UV-C16.

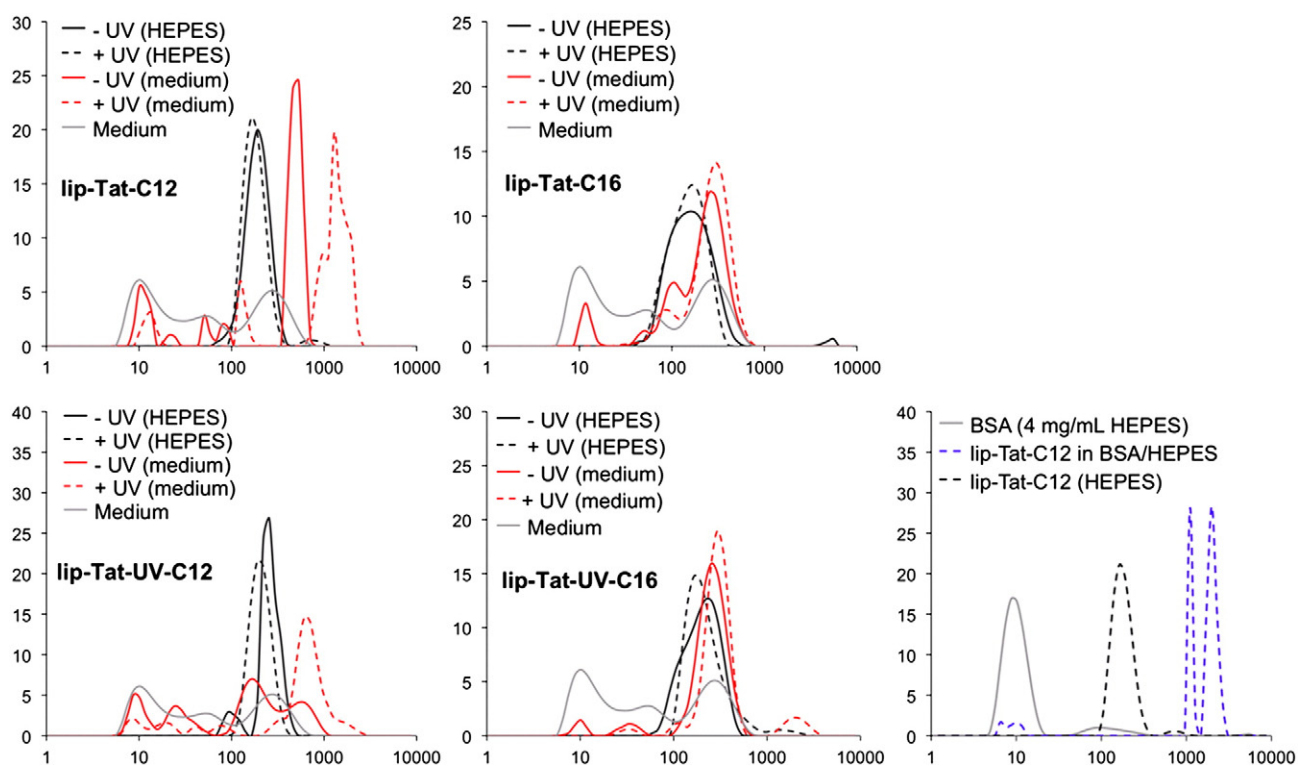


Fig. 5. Aggregation of Tat liposomes. Aggregation of lip-Tat-C12, lip-Tat-UV-C12-Tat, lip-Tat-C12 and lip-Tat-UV-C16 was monitored by dynamic light scattering in cell culture medium and in HEPES buffer.

4. Conclusions

Herein, we have described the synthesis of a UV-cleavable lipid anchor and demonstrated how this anchor can be used to constrain a cell-penetrating peptide (CPP) onto a liposomal surface. Further, we have shown that when the CPP was engaged in this loop formation no cellular adhesion or uptake did take place. However, upon irradiation opening of the loop and exposure of the CPP induced cellular adhesion and uptake. The next step will be to explore other triggers to release the constrained CPP such as enzymatic cleavage of the lipid anchor.

Acknowledgments

Louis van Bloois is acknowledged for assistance during liposome preparation. Prof. Joop van Zoelen, Inez Meijer and Walter van Rotterdam are thanked for their help with cell cultivation.

Appendix A. Supplementary data

Experimental details for the synthesis of the UV-cleavable anchors including characterization data. Characterization data of all the peptides. Additional confocal microscopy images. Supplementary data to this article can be found online at <http://dx.doi.org/10.1016/j.jconrel.2012.10.008>.

References

- [1] [Histones:]. K.M. Wagstaff, D.J. Glover, D.J. Tremethick, D.A. Jans, Histone-mediated transduction as an efficient means for gene delivery, *Mol. Ther.* 15 (4) (2007) 721–731.
- [2] [Silica:]. K. Patel, S. Angelos, W.R. Dichtel, A. Coskun, Y.-W. Yang, J.I. Zink, J.F. Stoddart, Enzyme-responsive snap-top covered silica nanocontainers, *J. Am. Chem. Soc.* 130 (8) (2008) 2382–2383.
- [3] [Amphiphilic dendrimers:]. M.A. Azagarsamy, P. Sokkalingam, S. Thayumanavan, Enzyme-triggered disassembly of dendrimer-based amphiphilic nanocontainers, *J. Am. Chem. Soc.* 131 (40) (2009) 14184–14185.
- [4] [Titaniumoxide:]. Y.-Y. Song, F. Schmidt-Stein, S. Bauer, P. Schmuki, Amphiphilic TiO₂ nanotube arrays: an actively controllable drug delivery system, *J. Am. Chem. Soc.* 131 (12) (2009) 4230–4232.
- [5] [Oligonucleotides:]. S.K. Taylor, R. Pei, B.C. Moon, S. Damera, A. Shen, M.N. Stojanovic, Triggered release of an active peptide conjugate from a DNA device by an orally administrable small molecule, *Angew. Chem. Int. Ed.* 48 (24) (2009) 4394–4397.
- [6] [Cyclodextrin:]. F. Versluis, I. Tomatsu, S. Kehr, C. Fregonese, A.W.J.W. Tepper, M.C.A. Stuart, B.J. Ravoo, R.I. Koning, A. Kros, Shape and release control of a peptide decorated vesicle through pH sensitive orthogonal supramolecular interactions, *J. Am. Chem. Soc.* 131 (37) (2009) 13186–13187.
- [7] [Yttrium:]. C.-J. Carling, F. Nourmohammadian, J.-C. Boyer, N.R. Branda, Remote-control photorelease of caged compounds using near-infrared light and upconverting nanoparticles, *Angew. Chem. Int. Ed.* 49 (22) (2010) 3782–3785.
- [8] [Peptides:]. L. Collins, A.L. Parker, J.D. Gehman, L. Eckley, M.A. Perugini, F. Separovic, J.W. Fabre, Self-assembly of peptides into spherical nanoparticles for delivery of hydrophilic moieties to the cytosol, *ACS Nano* 4 (5) (2010) 2856–2864.
- [9] [Amphiphilic polymers:]. D.M. Vriezema, J. Hoogboom, K. Velonia, K. Takazawa, P.C.M. Christianen, J.C. Maan, A.E. Rowan, R.J.M. Nolte, Vesicles and polymerized vesicles from thiophene-containing rod-coil block copolymers, *Angew. Chem. Int. Ed.* 42 (7) (2003) 772–776.
- [10] [Liposomes:]. V.P. Torchilin, R. Rammohan, V. Weissig, T.S. Levchenko, TAT peptide on the surface of liposomes affords their efficient intracellular delivery even at low temperature and in the presence of metabolic inhibitors, *Proc. Natl. Acad. Sci. U. S. A.* 98 (15) (2001) 8786–8791.
- [11] [Carbon nanotubes:]. S. Dhar, Z. Liu, J. Thomale, H. Dai, S.J. Lippard, Targeted single-wall carbon nanotube-mediated Pt(IV) prodrug delivery using folate as a homing device, *J. Am. Chem. Soc.* 130 (34) (2008) 11467–11476.
- [12] [Graphene oxide:]. Z. Liu, J.T. Robinson, X. Sun, H. Dai, PEGylated nanographene oxide for delivery of water-insoluble cancer drugs, *J. Am. Chem. Soc.* 130 (33) (2008) 10876–10877.
- [13] R.M. Straubinger, K. Hong, D.S. Friend, D. Papahadjopoulos, Endocytosis of liposomes and intracellular fate of encapsulated molecules: encounter with a low pH compartment after internalization in coated vesicles, *Cell* 32 (4) (1983) 1069–1079.
- [14] P.G. Tardi, N.L. Boman, P.R. Cullis, Liposomal doxorubicin, *J. Drug Target.* 4 (3) (1996) 129–140.
- [15] S. Zalipsky, N. Mullah, J.A. Harding, J. Gittelman, L. Guo, S.A. DeFrees, Poly(ethylene glycol)-grafted liposomes with oligopeptide or oligosaccharide ligands appended to the termini of the polymer chains, *Bioconjug. Chem.* 8 (2) (1997) 111–118.

- [16] M.M. Fretz, A. Høgset, G.A. Koning, W. Jiskoot, G. Storm, Cytosolic delivery of liposomally targeted proteins induced by photochemical internalization, *Pharm. Res.* 24 (11) (2007) 2040–2047.
- [17] F.M. Muggia, Liposomal encapsulated anthracyclines: new therapeutic horizons, *Curr. Oncol. Rep.* 3 (2) (2001) 156–162.
- [18] V.P. Torchilin, Recent advances with liposomes as pharmaceutical carriers, *Nat. Rev. Drug Discovery* 4 (2) (2005) 145–160.
- [19] US Food and Drug Administration, F.D.A., http://www.accessdata.fda.gov/drugsatfda_docs/label/2008/050718s033bl.pdf [accessed April 10, 2012].
- [20] T.M. Allen, C. Hansen, F. Martin, C. Redemann, A. Yau-Young, Liposomes containing synthetic lipid derivatives of poly(ethylene glycol) show prolonged circulation half-lives in vivo, *Biochim. Biophys. Acta* 1066 (1) (1991) 29–36.
- [21] G. Blume, G. Cevc, Liposomes for the sustained drug release in vivo, *Biochim. Biophys. Acta* 1029 (1) (1990) 91–97.
- [22] A.L. Klibanov, K. Maruyama, V.P. Torchilin, L. Huang, Amphipathic polyethyleneglycols effectively prolong the circulation time of liposomes, *FEBS Lett.* 268 (1) (1990) 235–237.
- [23] D. Papahadjopoulos, T.M. Allen, A. Gabizon, E. Mayhew, K. Matthay, S.K. Huang, K.D. Lee, M.C. Woodle, D.D. Lasic, C. Redemann, Sterically stabilized liposomes: improvements in pharmacokinetics and antitumor therapeutic efficacy, *Proc. Natl. Acad. Sci. U. S. A.* 88 (24) (1991) 11460–11464.
- [24] J. Senior, C. Delgado, D. Fisher, C. Tilcock, G. Gregoriadis, Influence of surface hydrophilicity of liposomes on their interaction with plasma protein and clearance from the circulation: studies with poly(ethylene glycol)-coated vesicles, *Biochim. Biophys. Acta* 1062 (1) (1991) 77–82.
- [25] S. Giri, B.G. Trewyn, M.P. Stellmaker, V.S.-Y. Lin, Stimuli-responsive controlled-release delivery system based on mesoporous silica nanorods capped with magnetic nanoparticles, *Angew. Chem. Int. Ed.* 44 (32) (2005) 5038–5044.
- [26] T.D. Nguyen, Y. Liu, S. Saha, K.C.-F. Leung, J.F. Stoddart, J.I. Zink, Design and optimization of molecular nanovalves based on redox-switchable bistable rotaxanes, *J. Am. Chem. Soc.* 129 (3) (2007) 626–634.
- [27] S. Dromi, V. Frenkel, A. Luk, B. Traugher, M. Angstadt, M. Bur, J. Poff, J. Xie, S.K. Libutti, K.C.P. Li, B.J. Wood, Pulsed-high intensity focused ultrasound and low temperature-sensitive liposomes for enhanced targeted drug delivery and antitumor effect, *Clin. Cancer Res.* 13 (9) (2007) 2722–2727.
- [28] R. Suzuki, Y. Oda, N. Utoguchi, E. Namai, Y. Taira, N. Okada, N. Kadowaki, T. Kodama, K. Tachibana, K. Maruyama, A novel strategy utilizing ultrasound for antigen delivery in dendritic cell-based cancer immunotherapy, *J. Control. Release* 133 (3) (2009) 198–205.
- [29] S. Mizukami, M. Hosoda, T. Satake, S. Okada, Y. Hori, T. Furuta, K. Kikuchi, Photocontrolled compound release system using caged antimicrobial peptide, *J. Am. Chem. Soc.* 132 (28) (2010) 9524–9525.
- [30] A. Koçer, M. Walko, W. Meijberg, B.L. Feringa, A light-actuated nanovalve derived from a channel protein, *Science* 309 (5735) (2005) 755–758.
- [31] B. Chandra, R. Subramaniam, S. Mallik, D.K. Srivastava, Formulation of photocleavable liposomes and the mechanism of their content release, *Org. Biomol. Chem.* 4 (9) (2006) 1730–1740.
- [32] S. Angelos, E. Choi, F. Vögtle, L. De Cola, J.I. Zink, Photo-driven expulsion of molecules from mesostructured silica nanoparticles, *J. Phys. Chem. C* 111 (18) (2007) 6589–6592.
- [33] Z. Li, Y. Wan, A.G. Kutateladze, Dithiane-based photolabile amphiphiles: toward photolabile liposomes, *Langmuir* 19 (16) (2003) 6381–6391.
- [34] J.L. Vivero-Escoto, I.I. Slowing, C.-W. Wu, V.S.-Y. Lin, Photoinduced intracellular controlled release drug delivery in human cells by gold-capped mesoporous silica nanosphere, *J. Am. Chem. Soc.* 131 (10) (2009) 3462–3463.
- [35] A.A. Kale, V.P. Torchilin, “Smart” drug carriers: PEGylated TATp-modified pH-sensitive liposomes, *J. Liposome Res.* 17 (3–4) (2007) 197–203.
- [36] A.A. Kale, V.P. Torchilin, Enhanced transfection of tumor cells in vivo using “Smart” pH-sensitive TAT-modified pegylated liposomes, *J. Drug Target.* 15 (7–8) (2007) 538–545.
- [37] R.M. Sawant, J.P. Hurlley, S. Salmaso, A. Kale, E. Tolcheva, T.S. Levchenko, V.P. Torchilin, “SMART” drug delivery systems: double-targeted pH-responsive pharmaceutical nanocarriers, *Bioconjug. Chem.* 17 (4) (2006) 943–949.
- [38] A.A. Kale, V.P. Torchilin, Design, synthesis, and characterization of pH-sensitive PEG-PE conjugates for stimuli-sensitive pharmaceutical nanocarriers: the effect of substituents at the hydrazine linkage on the pH stability of PEG-PE conjugates, *Bioconjug. Chem.* 18 (2) (2007) 363–370.
- [39] L. Jabr-Milane, L. van Vlerken, H. Devalapally, D. Shenoy, S. Komareddy, M. Bhavsar, M. Amiji, Multi-functional nanocarriers for targeted delivery of drugs and genes, *J. Control. Release* 130 (2) (2008) 121–128.
- [40] D. Schmaljohann, Thermo- and pH-responsive polymers in drug delivery, *Adv. Drug Delivery Rev.* 58 (15) (2006) 1655–1670.
- [41] G.A. Koning, A.M.M. Eggermont, L.H. Lindner, T.L.M. ten Hagen, Hyperthermia and thermosensitive liposomes for improved delivery of chemotherapeutic drugs to solid tumors, *Pharm. Res.* 27 (8) (2010) 1750–1754.
- [42] B. Smith, I. Lyakhov, K. Loomis, D. Needle, U. Baxa, A. Yavlovich, J. Capala, R. Blumenthal, A. Puri, Hyperthermia-triggered intracellular delivery of anticancer agent to HER2(+) cells by HER2-specific affibody (ZHER2-GS-Cys)-conjugated thermosensitive liposomes (HER2(+) affisomes), *J. Control. Release* 153 (2) (2011) 187–194.
- [43] M.B. Yatvin, J.N. Weinstein, W.H. Dennis, R. Blumenthal, Design of liposomes for enhanced local release of drugs by hyperthermia, *Science* 202 (4374) (1978) 1290–1293.
- [44] M.N. Antipina, G.B. Sukhorukov, Remote control over guidance and release properties of composite polyelectrolyte based capsules, *Adv. Drug Delivery Rev.* 63 (9) (2011) 716–729.
- [45] C. Foged, H.M. Nielsen, S. Frokjaer, Phospholipase A2 sensitive liposomes for delivery of small interfering RNA (siRNA), *J. Liposome Res.* 17 (3–4) (2007) 191–196.
- [46] A.I. Elegbede, J. Banerjee, A.J. Hanson, S. Tobwala, B. Ganguli, R. Wang, X. Lu, D.K. Srivastava, S. Mallik, Mechanistic studies of the triggered release of liposomal contents by matrix metalloproteinase-9, *J. Am. Chem. Soc.* 130 (32) (2008) 10633–10642.
- [47] S.C. Davis, F.C. Szoka, Cholesterol phosphate derivatives: synthesis and incorporation into a phosphatase and calcium-sensitive triggered release liposome, *Bioconjug. Chem.* 9 (6) (1998) 783–792.
- [48] S. Ganta, H. Devalapally, A. Shahiwala, M. Amiji, A review of stimuli-responsive nanocarriers for drug and gene delivery, *J. Control. Release* 126 (3) (2008) 187–204.
- [49] M. Calderera-Moore, N. Guimard, L. Shi, K. Roy, Designer nanoparticles: incorporating size, shape and triggered release into nanoscale drug carriers, *Expert Opin. Drug Deliv.* 7 (4) (2010) 479–495.
- [50] Y. Shamay, L. Adar, G. Ashkenasy, A. David, Light induced drug delivery into cancer cells, *Biomaterials* 32 (5) (2011) 1377–1386.
- [51] P. Xu, E. Gullotti, L. Tong, C.B. Highley, D.R. Errabelli, T. Hasan, J.-X. Cheng, D.S. Kohane, Y. Yeo, Intracellular drug delivery by poly(lactic-co-glycolic acid) nanoparticles, revisited, *Mol. Pharm.* 6 (1) (2009) 190–201.
- [52] K. Riehemann, S.W. Schneider, T.A. Luger, B. Godin, M. Ferrari, H. Fuchs, Nanomedicine—challenge and perspectives, *Angew. Chem. Int. Ed.* 48 (5) (2009) 872–897.
- [53] R. Xiong, Z. Li, L. Mi, P.-N. Wang, J.-Y. Chen, L. Wang, W.-L. Yang, Study on the intracellular fate of Tat peptide-conjugated quantum dots by spectroscopic investigation, *J. Fluoresc.* 20 (2) (2010) 551–556.
- [54] H. Yukawa, Y. Kagami, M. Watanabe, K. Oishi, Y. Miyamoto, Y. Okamoto, M. Tokeshi, N. Kaji, H. Noguchi, K. Ono, M. Sawada, Y. Baba, N. Hamajima, S. Hayashi, Quantum dots labeling using octa-arginine peptides for imaging of adipose tissue-derived stem cells, *Biomaterials* 31 (14) (2010) 4094–4103.
- [55] S.F.M. van Dongen, W.P.R. Verdurmen, R.J.R.W. Peters, R.J.M. Nolte, R. Brock, J.C.M. van Hest, Cellular integration of an enzyme-loaded polymersome nanoreactor, *Angew. Chem. Int. Ed.* 49 (40) (2010) 7213–7216.
- [56] M.M. Fretz, G.A. Koning, E. Mastrobattista, W. Jiskoot, G. Storm, OVCAR-3 cells internalize TAT-peptide modified liposomes by endocytosis, *Biochim. Biophys. Acta* 1665 (1–2) (2004) 48–56.
- [57] L. Chaloin, P. Bigey, C. Loup, M. Marin, N. Galeotti, M. Piechaczyk, F. Heitz, B. Meunier, Improvement of porphyrin cellular delivery and activity by conjugation to a carrier peptide, *Bioconjug. Chem.* 12 (5) (2001) 691–700.
- [58] R. Fischer, M. Fotin-Mleczek, H. Hufnagel, R. Brock, Break through to the other side—biophysics and cell biology shed light on cell-penetrating peptides, *ChemBioChem* 6 (12) (2005) 2126–2142.
- [59] K.M. Stewart, K.L. Horton, S.O. Kelley, Cell-penetrating peptides as delivery vehicles for biology and medicine, *Org. Biomol. Chem.* 6 (13) (2008) 2242–2255.
- [60] N. Schmidt, A. Mishra, G.H. Lai, G.C.L. Wong, Arginine-rich cell-penetrating peptides, *FEBS Lett.* 584 (9) (2010) 1806–1813.
- [61] V.P. Torchilin, Tatp-mediated intracellular delivery of pharmaceutical nanocarriers, *Biochem. Soc. Trans.* 35 (Pt 4) (2007) 816–820.
- [62] D. Sarko, B. Beijer, R.G. Boy, E.M. Nothelfer, K. Leotta, M. Eisenhut, A. Altmann, U. Haberkorn, W. Mier, The pharmacokinetics of cell-penetrating peptides, *Mol. Pharm.* 7 (6) (2010) 2224–2231.
- [63] M. Kosuge, T. Takeuchi, I. Nakase, A.T. Jones, S. Futaki, Cellular internalization and distribution of arginine-rich peptides as a function of extracellular peptide concentration, serum, and plasma membrane associated proteoglycans, *Bioconjug. Chem.* 19 (3) (2008) 656–664.
- [64] G. Breipohl, J. Knolle, W. Stüber, Synthesis and application of acid labile anchor groups for the synthesis of peptide amides by Fmoc-solid-phase peptide synthesis, *Int. J. Pept. Protein Res.* 34 (4) (1989) 262–267.
- [65] W. Stüber, J. Knolle, G. Breipohl, Synthesis of peptide amides by Fmoc-solid-phase peptide synthesis and acid labile anchor groups, *Int. J. Pept. Protein Res.* 34 (3) (1989) 215–221.
- [66] G.B. Fields, R.L. Noble, Solid phase peptide synthesis utilizing 9-fluorenylmethoxycarbonyl amino acids, *Int. J. Pept. Protein Res.* 35 (1990) 161–214.
- [67] E. Kaiser, R.L. Colescott, C.D. Bossinger, P.I. Cook, Color test for detection of free terminal amino groups in the solid-phase synthesis of peptides, *Anal. Biochem.* 34 (1970) 595–598.
- [68] F. Szoka, D. Papahadjopoulos, Procedure for preparation of liposomes with large internal aqueous space and high capture by reverse-phase evaporation, *Proc. Natl. Acad. Sci. U. S. A.* 75 (9) (1978) 4194–4198.
- [69] G. Rouser, S. Fkeischer, A. Yamamoto, Two dimensional thin layer chromatographic separation of polar lipids and determination of phospholipids by phosphorus analysis of spots, *Lipids* 5 (5) (1970) 494–496.
- [70] A.D. Frankel, C.O. Pabo, Cellular uptake of the tat protein from human immunodeficiency virus, *Cell* 55 (6) (1988) 1189–1193.
- [71] M. Green, P.M. Loewenstein, Autonomous functional domains of chemically synthesized human immunodeficiency virus tat trans-activator protein, *Cell* 55 (6) (1988) 1179–1188.
- [72] E. Mastrobattista, G.A. Koning, L. van Bloois, A.C.S. Filipe, W. Jiskoot, G. Storm, Functional characterization of an endosome-disruptive peptide and its application in cytosolic delivery of immunoliposome-entrapped proteins, *J. Biol. Chem.* 277 (30) (2002) 27135–27143.
- [73] H.B. Lee, M.C. Zaccaro, M. Pattarawarapan, S. Roy, H.U. Saragovi, K. Burgess, Syntheses and activities of new C10 beta-turn peptidomimetics, *J. Org. Chem.* 69 (3) (2004) 701–713.
- [74] A.A. Spector, K. John, J.E. Fletcher, Binding of long-chain fatty acids to bovine serum albumin, *J. Lipid Res.* 10 (1) (1969) 56.